# $GABA_A$-Mediated IPSCs in Piriform Cortex Have Fast and Slow Components With Different Properties and Locations on Pyramidal Cells

A. KAPUR,[1] R. A. PEARCE,[1,2] W. W. LYTTON,[1,3] AND L. B. HABERLY[1,4]
[1]*Neuroscience Program,* [2]*Department of Anesthesiology,* [3]*Department of Neurology, and* [4]*Department of Anatomy, University of Wisconsin, Madison, Wisconsin 53706*

**Kapur, A., R. A. Pearce, W. W. Lytton, and L. B. Haberly.** $GABA_A$-mediated IPSCs in piriform cortex have fast and slow components with different properties and locations on pyramidal cells. *J. Neurophysiol.* 78: 2531–2545, 1997. A recent study in piriform (olfactory) cortex provided evidence that, as in hippocampus and neocortex, $\gamma$-aminobutyric acid-A ($GABA_A$)-mediated inhibition is generated in dendrites of pyramidal cells, not just in the somatic region as previously believed. This study examines selected properties of $GABA_A$ inhibitory postsynaptic currents (IPSCs) in dendritic and somatic regions that could provide insight into their functional roles. Pharmacologically isolated $GABA_A$-mediated IPSCs were studied by whole cell patch recording in slices. To compare properties of IPSCs in distal dendritic and somatic regions, local stimulation was carried out with tungsten microelectrodes, and spatially restricted blockade of $GABA_A$-mediated inhibition was achieved by pressure-ejection of bicuculline from micropipettes. The results revealed that largely independent circuits generate $GABA_A$ inhibition in distal apical dendritic and somatic regions. With such independence, a selective decrease in dendritic-region inhibition could enhance integrative or plastic processes in dendrites while allowing feedback inhibition in the somatic region to restrain system excitability. This could allow modulatory fiber systems from the basal forebrain or brain stem, for example, to change the functional state of the cortex by altering the excitability of interneurons that mediate dendritic inhibition without increasing the propensity for regenerative bursting in this highly epileptogenic system. As in hippocampus, $GABA_A$-mediated IPSCs were found to have fast and slow components with time constants of decay on the order of 10 and 40 ms, respectively, at 29°C. Modeling analysis supported physiological evidence that the slow time constant represents a true IPSC component rather than an artifactual slowing of the fast component from voltage clamp of a dendritic current. The results indicated that, whereas both dendritic and somatic-region IPSCs have both fast and slow $GABA_A$ components, there is a greater proportion of the slow component in dendrites. In a companion paper, the hypothesis is explored that the resulting slower time course of the dendritic IPSC increases its capacity to regulate the *N*-methyl-D-aspartate component of EPSPs. Finally, evidence is presented that the slow $GABA_A$-mediated IPSC component is regulated by presynaptic $GABA_B$ inhibition whereas the fast is not. Based on the requirement for presynaptic $GABA_B$-mediated block of inhibition for expression of long-term potentiation, this finding is consistent with participation of the slow $GABA_A$ component in regulation of synaptic plasticity. The lack of susceptibility of the fast $GABA_A$ component to the long-lasting, activity-induced suppression mediated by presynaptic $GABA_B$ receptors is consistent with a protective role for this process in preventing seizure activity.

## INTRODUCTION

For several decades after its discovery, the study of inhibition mediated by $\gamma$-aminobutyric acid-A ($GABA_A$) receptors largely consisted of confirmation in many systems that it is generated in or near cell bodies by feedback pathways. In recent years, however, it has become apparent that $GABA_A$-mediated inhibition in the cerebral cortex is a complex process that is generated in dendrites as well as cell bodies (Buhl et al. 1994a; Lambert et al. 1991; Miles et al. 1996; Pearce 1993), has fast and slow components (Pearce 1993), and is regulated by diverse mechanisms. A thorough knowledge of GABAergic processes clearly will be required for understanding a wide variety of neuronal functions including the integration of spatially and temporally patterned inputs, the regulation of relationships between inputs and output, the coupling of activity to learning-related changes in synaptic efficacy, and maintenance of the intricate balances between excitation and inhibition that are required for optimal function while minimizing the risk of seizure activity.

As in other brain areas, early studies in piriform cortex provided anatomic and physiological evidence that there is strong somatic-region $GABA_A$-mediated inhibition generated through a feedback pathway (Biedenbach and Stevens 1969; Haberly 1973; Satou et al. 1983). More recently, evidence from a study of modulation of the *N*-methyl-D-aspartate (NMDA) component of excitatory postsynaptic potentials (EPSPs) indicated that $GABA_A$ inhibition also is generated in apical dendrites of piriform pyramidal cells (Kanter et al. 1996) as in other types of cerebral cortex. The results of that study indicated that even though the dendritic $GABA_A$ inhibitory postsynaptic potential (IPSP) is small in somatic recordings, it can strongly regulate expression of the NMDA component. Because NMDA-dependent long-term potentiation (LTP) in piriform cortex is regulated by $GABA_A$ inhibition (del Cerro et al. 1992; Kanter and Haberly 1993) as in other types of cerebral cortex, this finding suggests that dendritic inhibition may play a role in controlling synaptic plasticity.

The present study was undertaken to confirm that $GABA_A$-mediated inhibition is present in distal dendritic as well as somatic regions of pyramidal cells in piriform cortex as in hippocampus and neocortex and to determine if there are differences in properties in these different regions that may assist in understanding their roles in normal function and epileptogenesis. The analysis was guided by three hypotheses: that inhibitory circuitry impinging on dendritic and somatic regions is separate, that fast and slow $GABA_A$ components are present in piriform cortex with the slow expressed

0022-3077/97 $5.00 Copyright © 1997 The American Physiological Society 

to a greater extent in dendrites than cell bodies, and that the slow component preferentially is subject to regulation by presynaptic $GABA_B$ inhibition.

The prediction that inhibitory circuitry for dendritic and somatic regions is separate stems from the fact that even partial indiscriminate disinhibition in piriform cortex, as in most cortical areas, evokes epileptiform bursting (Kanter and Haberly 1993), and evidence that feedback inhibition in the vicinity of cell bodies is largely responsible for prevention of such bursting through control of cell firing (Miles et al. 1996; Traub et al. 1987). If dendritic and somatic region inhibitory systems are separate in piriform cortex as in the hippocampus (Freund and Buzaki 1996), selective block of the dendritic component for purposes of enabling dendritic processes such as NMDA-dependent LTP would be possible during normal function. Separation also could allow feedback adjustments in system excitability through changes in the strength of somatic-region inhibition with minimal effect on integrative processes (see Kapur et al. 1997).

The prediction that a slow $GABA_A$-mediated IPSC component is present in piriform cortex and expressed to a greater degree in dendrites as in hippocampus (Pearce 1993), stems from the hypothesis that a slower dendritic inhibitory postsynaptic current (IPSC) would exert a stronger controlling action on the NMDA component by virtue of a better match in time course (see Kapur et al. 1997).

The final prediction, that the slow $GABA_A$ component is selectively regulated by presynaptic $GABA_B$ receptors is based on the assumption that, as in hippocampus (Davies et al. 1991; Mott and Lewis 1991), the induction of NMDA-dependent LTP in piriform cortex requires activity-dependent blockade of $GABA_A$ inhibition. Selective susceptibility of the slow $GABA_A$ component to the long-lasting suppression mediated by presynaptic $GABA_B$ receptors as demonstrated in hippocampus (Pearce et al. 1995) could serve to protect the system from regenerative bursting that might develop if the fast component also were subject to prolonged interruption.

The results provided a direct demonstration that $GABA_A$-mediated IPSCs are generated in dendrites of pyramidal cells in piriform cortex and verified the three predictions concerning properties of $GABA_A$ inhibition in dendritic and somatic regions. These findings are used in a companion paper to explore the hypothesis stemming from recent experimental findings (Kanter et al. 1997) that the differing properties of dendritic and somatic IPSCs provide a physiologically reasonable mechanism for control of the NMDA component and other dendritic processes through a differential regulation of IPSCs in these two regions.

## METHODS

Slices were prepared from the piriform cortex of 3- to 4-wk-old male Sprague Dawley rats. Decapitation was under ether anesthesia. Slices were cut perpendicular to the cortical surface by making a small adjustment in block-face orientation relative to the coronal plane to preserve as much of the dendritic trees of pyramidal cells as possible. Sectioning was carried out with a Vibratome (Lancer) at 500 $\mu$m thickness in carbogen-saturated artificial cerebrospinal fluid at ~4°C. This medium contained (in mM) 126 NaCl, 3 KCl, 2 $CaCl_2$, 1 $MgSO_4$, 1.25 $NaH_2PO_4$, 26 $NaHCO_3$, and 10 D-glucose

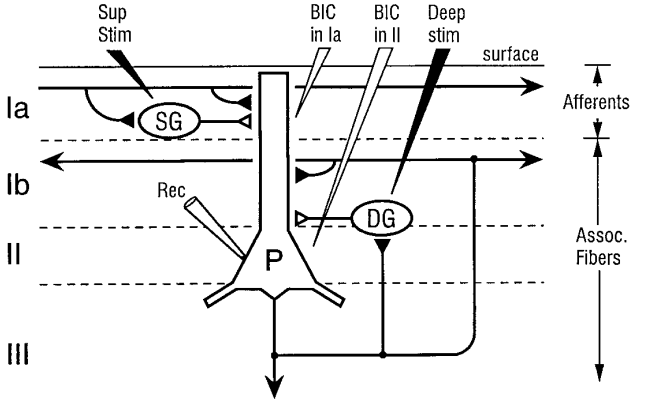


FIG. 1. Lamination of piriform cortex, excitatory inputs to pyramidal cells, postulated inhibitory circuitry, and placement of electrodes. Cell bodies of superficial pyramidal cells (P) are in layer II; their apical dendrites extend into layer I and basal dendrites into layer III. Afferent fibers from the olfactory bulb are confined to layer Ia; association fibers (recurrent collaterals of pyramidal cell axons) are in layers Ib and III and, to a lesser extent, layer II. Afferent fibers synapse on distal segments of pyramidal cell apical dendrites; association fibers synapse on proximal segments of pyramidal cell apical dendrites in layer Ib and basal dendrites in layer III (not shown). Postulated superficial (SG) and deep (DG) GABAergic interneurons synapse on apical dendritic and somatic regions of pyramidal cells, respectively. Recording was with a patch pipette (REC) from cell bodies of layer II pyramidal cells. One stimulating electrode was placed in superficial Ia (Sup Stim) to activate inhibitory circuitry in the distal dendritic region, and 1 in the association fiber layers in Ib, II, or superficial III (Deep Stim) to activate inhibitory circuitry in the somatic region. $\gamma$-aminobutyric acid-A ($GABA_A$)-mediated inhibition was blocked locally by pressure injection from bicuculline-containing pipettes in the distal dendritic (BIC in Ia) or somatic region (BIC in II) of the patched neuron.

and was equilibrated with 95% $O_2$-5% $CO_2$. Osmolarity was 320 mOsm.

Recordings were made at 29 ± 1°C in submerged slices perfused with oxygenated medium circulating at ~45 ml/h in the chamber described by Tseng and Haberly (1988). Darkfield illumination through a transparent base allowed visualization of all layers. Recordings were made in layer II using the blind whole cell patch technique (Blanton et al. 1989). Pipette resistances were 7–12 MΩ in the extracellular space; tips were coated with Sigmacote (Sigma) to lower capacitance. Adequate voltage clamp could be attained when series resistance was <30 MΩ. Recordings were made with an Axoclamp-2A amplifier in discontinuous voltage clamp mode. Headstage output was monitored with a separate oscilloscope to assure adequate settling time. Switching frequency was 5 kHz in most experiments. Recording pipettes contained (in mM) 135 Cs-gluconate, 2 $MgCl_2$, 0.5 $CaCl_2$, 10 *N*-[2-hydroxyethyl]piperazine-*N*′-[2-ethanesulfonic acid] (sodium salt), 5 ethylene glycol-bis($\beta$-aminoethylether) *N*,*N*,*N*′,*N*′-tetraacetic acid, 2 ATP (ATP, Mg salt), and 5 lidocaine N-ethyl bromide (QX-314). The solution was buffered with CsOH to pH 7.3; final osmolarity was 290–330 mOsm. With $Cs^+$-containing pipettes, resting potential was approximately −45 mV. Cells were typically held at −35 mV to increase the driving force on IPSCs. Responses were recorded and analyzed with pClamp v 5.5 (Axon Instruments). Time constants of IPSCs were determined with the simplex routine provided in pClamp (Axon Instruments). The junction potential at the pipette tip (12 mV), measured as described by Neher (1992), was subtracted from responses.

Neuronal circuitry in piriform cortex is summarized in Fig. 1. Afferent fibers terminate on distal apical dendrites of pyramidal cells in layer Ia. Axons that originate from pyramidal cells, termed association fibers, course through layers Ib, II, and III and are excluded from layer Ia. These axons synapse on proximal dendrites

of pyramidal cells in layer Ib and basal dendrites in layer III. The superficial and deep GABAergic interneurons that are postulated to terminate on apical dendrites and cell bodies, respectively, are illustrated in layers Ia and II.

Axons were stimulated with 0.1 ms shocks delivered every 10–30 s using pairs of tungsten microelectrodes (5 MΩ, A-M Systems) placed under direct vision. One electrode was placed in the layer to be stimulated, the other nearby to create a bipolar stimulus.

Focal block of $GABA_A$-mediated IPSCs was accomplished by pressure-ejection of 1 mM bicuculline methiodide from broken-tip micropipettes. Tips of injection pipettes were 3–5 $\mu$m in diameter (OD); pressure was typically 30 psi; duration of pressure pulses was 10–40 ms.

3-amino-propyl (diethoxymethyl) phosphinic acid (CGP 35348) was a gift from Ciba-Geigy; 6,7-dinitroquinoxaline-2,3-dione (DNQX), R(+)-baclofen, and QX-314 were obtained from Research Biochemicals; D,L-2-amino-5-phosphonovaleric acid (D,L-APV) and bicuculline methiodide were from Sigma; D-APV was from Cambridge Research Biochemicals.

Data are expressed as means ± SE. Statistical comparisons are two-tailed *t*-tests (1 group or paired, as specified).

## RESULTS

Pharmacologically isolated monosynaptic $GABA_A$-mediated IPSCs were evoked in layer II pyramidal cells by stimulation of inhibitory cells and their axons at a distance of ~250 $\mu$m from the recording site. Glutamatergic excitatory postsynaptic currents and polysynaptic IPSCs were blocked by bath-applied DNQX (20 $\mu$M) and APV (15 $\mu$M D-APV or 30 $\mu$M D,L-APV) and $GABA_B$-mediated IPSCs blocked by $Cs^+$ (135 mM) and QX-314 (5 mM) in the recording pipette. IPSCs were evoked from a ''superficial'' tungsten microelectrode in layer Ia and from a ''deep'' tungsten microelectrode in layer Ib, layer II, or the superficial part of layer III (Fig. 1). No differences were detected in results obtained with stimulation in layers Ib, II, or III. Bath application of 10 $\mu$M bicuculline reversibly blocked responses to both superficial and deep stimulation (Fig. 2), confirming that the pharmacological isolation of the $GABA_A$-mediated IPSC was complete.

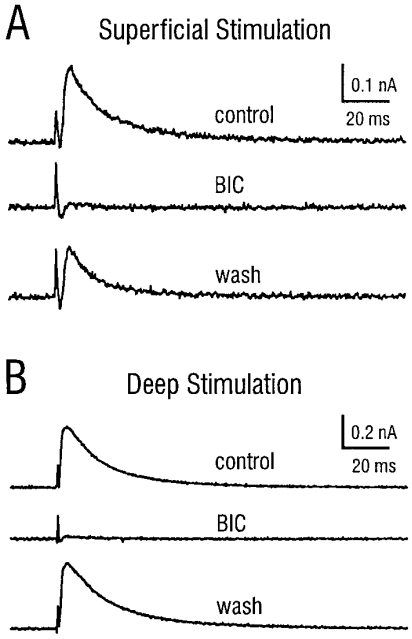


FIG. 2. Isolated $GABA_A$-mediated inhibitory postsynaptic currents (IPSCs) can be evoked by superficial (afferent layer) stimulation and deep (association fiber layer) stimulation after pharmacological blockade of glutamatergic excitatory postsynaptic currents (EPSCs). Responses in *A* and *B* are voltage-clamp, whole cell patch recordings from the soma of a layer II pyramidal cell. In this and all subsequent figures, EPSCs were blocked by bath applied 6,7-dinitroquinoxaline-2,3-dione (DNQX) and 2-amino-5-phosphonovaleric acid (APV). *A*: response to shock stimulation in the superficial part of layer Ia in DNQX and APV (control), after addition of 10 $\mu$M bicuculline (BIC), to confirm that the response in DNQX and APV was $GABA_A$-mediated and after washout of BIC (wash). *B*: same as *A*, but for deep stimulation (layer Ib). Holding potential in this and subsequent figures was depolarized with respect to the $GABA_A$ reversal, except as noted.

### *Laminar specificity of inhibitory circuitry*

To test the prediction that separate inhibitory circuits provide input to distal dendritic and somatic regions, the effects of focally applied bicuculline on IPSCs evoked from different layers were examined. Bicuculline methiodide was pressure ejected from micropipettes positioned either in the distal apical dendritic region or in the vicinity of the cell body of the neuron under study. Results from a typical experiment are illustrated in Fig. 3. When bicuculline was applied in layer Ia, the IPSC evoked by superficial stimulation was blocked by 60% before there was any effect on the IPSC evoked by deep stimulation (Fig. 3*A, 1* and *2*). A small decrease in deep response was observed but required 30 s to develop, indicating that few inhibitory axons activated by deep stimulation terminated at the site of bicuculline application. Conversely, when bicuculline was applied near the patched cell body in layer II, the deep-evoked IPSC was blocked by 80% when the superficial-evoked IPSC was blocked by 10% (Fig. 3*B, 1* and *2*). In this case, the latency of action on both deep and superficial responses was equally brief, suggesting that a small proportion of inhibitory axons activated from the superficial site terminated in the vicinity of bicuculline application in layer II.

In pooled data from experiments in which the goal was to achieve maximal differentiation, application of bicuculline in layer Ia blocked the superficial-evoked IPSC by 50 ± 5% at a time when it blocked the deep-evoked IPSC by 8 ± 4% ($n = 7$, $P < 0.001$, paired *t*-test; Fig. 3*A3*). In contrast, application of bicuculline near the soma blocked the superficial-evoked IPSC by 11 ± 2% when the deep-evoked IPSC was blocked by 66 ± 5% ($n = 6$, $P < 0.0001$; Fig. 3*B3*). Application of bicuculline in the basal dendritic region (layer III; not illustrated) blocked IPSCs evoked by deep stimulation but not IPSCs evoked by superficial stimulation as observed with application in layer II. Injection of bicuculline in the mid-apical region (layer Ib) (not illustrated) simultaneously blocked IPSCs evoked from both superficial and deep stimulation. It is unclear to what extent this reflects a lack of segregation of inputs in the mid-apical region as opposed to diffusion of bicuculline to both distal dendrites and cell bodies.

The results indicate that IPSCs evoked by superficial stimulation are generated predominantly in distal apical dendrites, whereas those evoked from deep stimulation are concentrated in the vicinity of the cell body and basal dendrites.

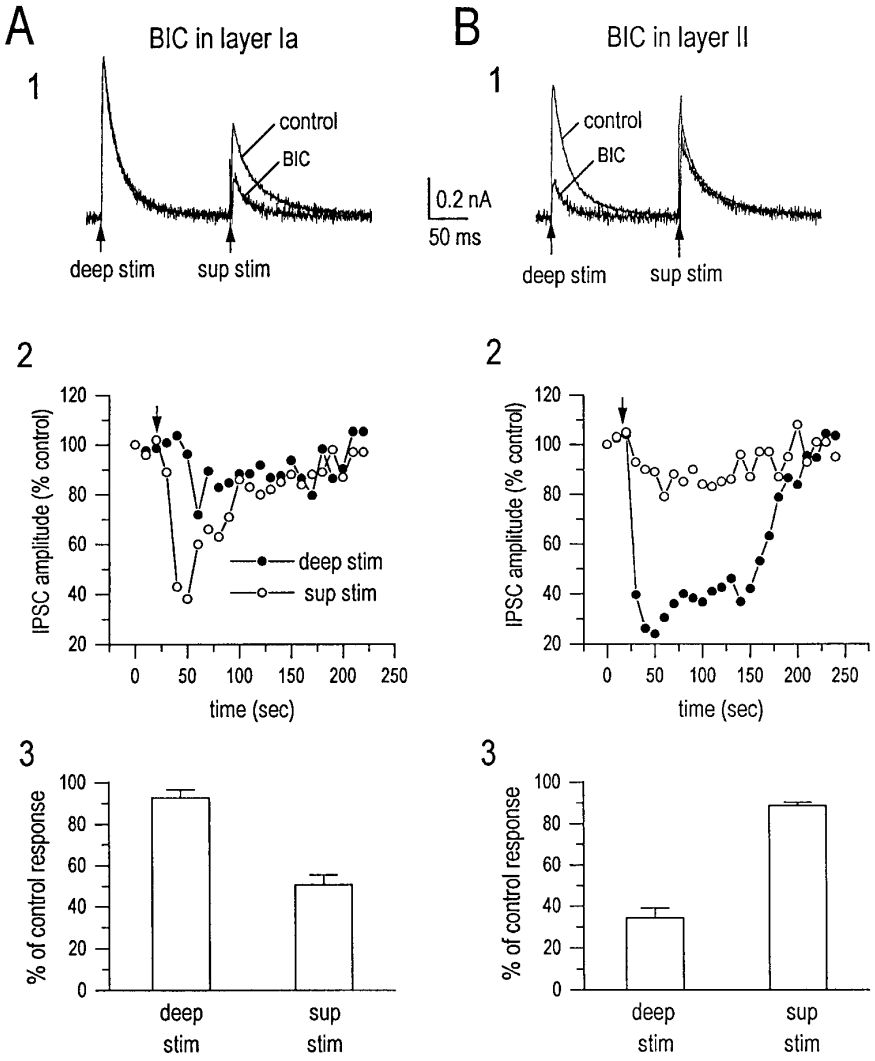


FIG. 3. The IPSC evoked by superficial stimulation is concentrated in the distal apical dendrites of pyramidal cells, whereas the IPSC from deep stimulation is concentrated near cell bodies. $GABA_A$-mediated IPSCs were recorded from cell bodies as described for Fig. 2. *A*: effect of local application of bicuculline (BIC) in layer Ia on the $GABA_A$-mediated IPSC evoked by deep and superficial (sup) stimulation. *B*: effect of bicuculline applied near the cell body in layer II. *A1* and *B1*: superimposed responses to superficial (layer Ia) and deep (layer III) stimulation, before and after application of bicuculline. With distal dendritic application (*A1*), the IPSC evoked by superficial stimulation was reduced by 60% at a time when the IPSC evoked by deep stimulation was unaffected. With somatic application (*B1*), the deep layer-evoked IPSC was blocked by 75% when the IPSC from superficial stimulation was reduced by 10%. *A2* and *B2*: amplitudes of IPSCs evoked by deep and superficial stimulation as a function of time after application of bicuculline. Control amplitudes are normalized to 100%. ↓, time of bicuculline application. *A3* and *B3*: mean amplitude of IPSCs evoked by deep and superficial stimulation in all experiments at the latency of maximal differentiation of the bicuculline effect (10–30 s postapplication). Error bars are SEs. Significance was $P < 0.001$ ($n = 7$) in *A*3; and $P < 0.0001$ ($n = 6$) in *B*3.

### *Kinetics of $GABA_A$-mediated IPSCs*

To determine if $GABA_A$-mediated IPSCs in piriform cortex consist of fast and slow components as in the hippocampus (Pearce 1993), the falling phase was fitted to exponential functions. The time course of decay of $GABA_A$-mediated IPSCs evoked from all layers was usually best fit by a sum of two exponentials: one with a ''fast'' time constant on the order of 10 ms, and one with a ''slow'' time constant on the order of 40 ms at 29°C (Fig. 4*A*). Fast and slow time constants for IPSCs evoked from different layers are summarized in Table 1. Fast and slow time constants remained well separated over a wide range of relative amplitudes (Fig. 4*C*).

Although both fast and slow components usually were present in IPSCs evoked from all layers, the proportion of slow component was larger in IPSCs evoked by superficial stimulation (layer Ia) than in IPSCs evoked from deep stimulation (Ib, II, or superficial III; Fig. 4). With superficial stimulation, the fast component contributed, on average, 57 ± 4% (range: 26–75%) (layer Ia in Table 1; Fig. 4*C*). For IPSCs evoked by deep stimulation, the contribution of the fast was 73 ± 3% fast (range 50–92%; average for layers Ib and III in Table 1; Fig. 4*C*; $P < 0.0001$ for superficial vs. deep, unpaired *t*-test). IPSCs with little or no slow component were evoked from a small number of deep sites, but there was a substantial proportion of fast component in all responses from superficial sites (Fig. 4*C*). This is in contrast to the hippocampus where IPSCs with no detectable fast or slow component were observed frequently (Pearce 1993).

### *Test for effects of imperfect space clamp*

Because the time course of synaptic currents in dendrites can be slowed when measured by voltage clamp at the cell body (Mainen et al. 1996; Major 1993; Rall and Segev 1985; Spruston et al. 1993), it could be argued that the slow IPSC component is artifactual. To determine if the slow component is kinetically distinct from the fast, the delayed voltage-clamp method of Pearce (1993) was applied. The objective was to test for the presence of an active synaptic conductance at a latency when the fast IPSC component would be minimal. Recorded cells were held at or near the reversal potential of the IPSC during shock stimulation of inhibitory axons to minimize current flow. The membrane potential was stepped to a more positive level at a series of latencies after the stimulus so that any synaptic conductance still active at that time would appear as an inward current. The brief

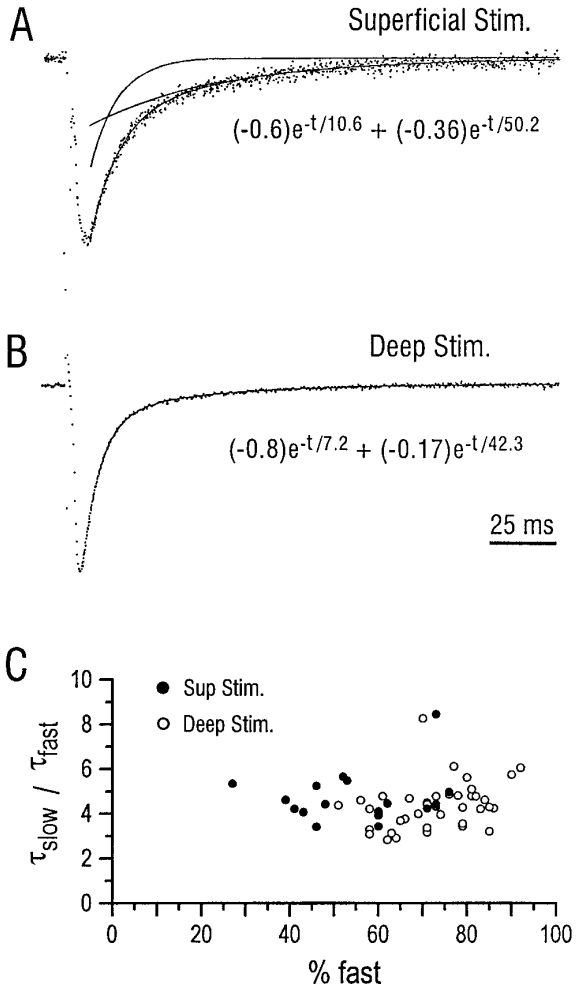


FIG. 4. $GABA_A$-mediated IPSCs decay with 2 time constants. *A*: isolated monosynaptic $GABA_A$-mediated IPSC evoked by superficial stimulation (layer Ia). Line through data points, best-fit biexponential function; the other solid lines are plots of the fast and slow components alone. Faster decaying component ($\tau$ = 10.6 ms) contributed 63% of the peak amplitude and the slower component ($\tau$ = 50.2 ms) contributed 37%. *B*: isolated monosynaptic $GABA_A$-mediated IPSC evoked by deep stimulation (deep part of layer Ib). Peak amplitude consisted of 82% fast ($\tau$ = 7.2 ms) and 18% slow ($\tau$ = 42.3 ms). Time scale in *B* also applies to *A*. Holding potential was hyperpolarized (−90 mV) with respect to $GABA_A$ reversal so that currents in *A* and *B* are inward. *C*: time constants of fast and slow components were well separated over a wide range of relative amplitudes. Values of $\tau_{slow}/\tau_{fast}$ for IPSCs recorded in 57 cells are plotted against the percent contribution of the fast component. ●, IPSCs evoked by superficial stimulation (layer Ia); ○, evoked by deep stimulation (Ib, II, or superficial III).

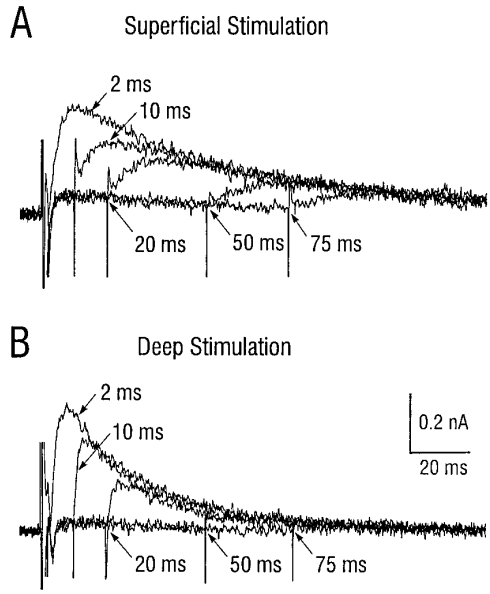


FIG. 5. Slow time constant of decay of the $GABA_A$-mediated IPSC represents a slowly decaying component of conductance. Membrane potential was held initially near the reversal potential of the IPSC (−52 mV) and subsequently stepped to a depolarized level (−32 mV) at a series of latencies after a shock in either layer Ia *(A)* or in layer III *(B)*. Synaptic currents observed on stepping the membrane potential away from the IPSC reversal at the various latencies after the stimulus have been overlaid. Capacitative currents resulting from the voltage step alone (no stimulus) were subtracted. Note that outward current is elicited by the voltage step at intervals of ≤75 ms for the response evoked from layer Ia, consistent with the presence of currents of synaptic origin at this latency.

capacitative transients resulting from the voltage step were subtracted digitally.

In the experiment illustrated in Fig. 5*A*, a synaptic current could be observed when the membrane potential was stepped from near the IPSC reversal potential (−52 mV) to −32 mV at latencies ≤75 ms after superficial stimulation. In contrast, no synaptic current was evoked by a voltage step at 75 ms in response to deep stimulation (Fig. 5*B*). Because little current could flow before the voltage step, the presence of current at 75 ms poststimulus suggests that an active synaptic conductance was present at that latency. A similar result was observed in 3/3 cells.

### *Laminar separation of fast and slow $GABA_A$ components*

The finding that IPSCs evoked by superficial and deep stimulation have different proportions of fast and slow components (Fig. 4), together with the evidence for laminar

TABLE 1. *Time constants of decay and relative amplitudes of fast and slow components of $GABA_A$-receptor mediated IPSCs evoked from different layers*

| Stimulus Site | $\tau_{fast}$ | $\tau_{slow}$ | $\tau_{slow}/\tau_{fast}$ | Percent Fast | *n* |
|---|---|---|---|---|---|
| | ms | | | | |
| Layer Ia | 10.3 ± 0.48 | 47.6 ± 2.8 | 4.61 ± 0.28 | 57 ± 4% | 17 |
| Layer Ib | 9 ± 0.41 | 38.4 ± 1.2 | 4.25 ± 0.18 | 71 ± 2% | 29 |
| Layer III | 11.2 ± 0.6 | 45.6 ± 3.3 | 4.09 ± 0.37 | 77 ± 4% | 11 |

Values are means ± SE.

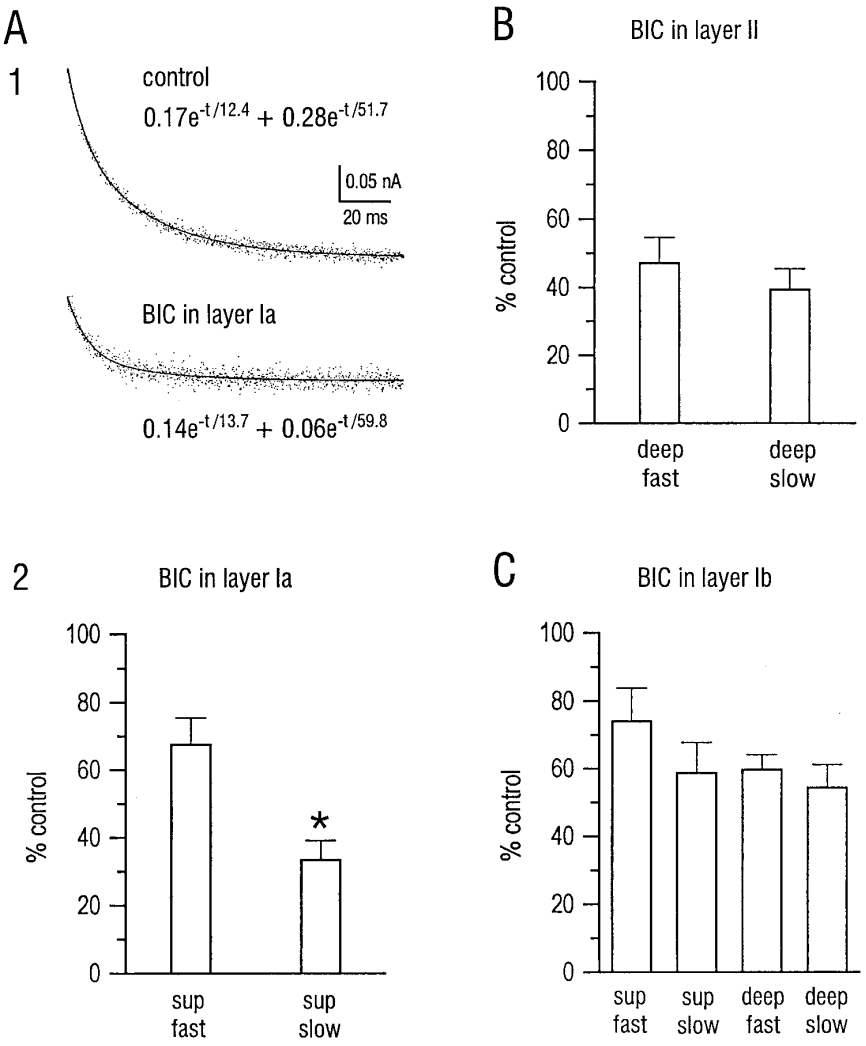


FIG. 6. Slow component of the IPSC evoked by superficial stimulation is blocked preferentially by application of bicuculline to the distal apical dendritic region. *A1*: sample responses from 1 experiment. Coefficients of the fast and slow components before (*top*) and after bicuculline (*bottom*) reveal changes in relative amplitude. *A2*: mean amplitudes (relative to control) of fast and slow components of IPSCs evoked by superficial (sup) stimulation after application of bicuculline to distal apical dendrites in layer Ia. Slow component was blocked to a greater extent than the fast (slow blocked by 67 ± 6%, fast by 33 ± 8%; $n = 7$, $P < 0.01$). Application of bicuculline near cell bodies in layer II *(B)* or to mid-apical dendrites in layer Ib *(C)* did not differentially block fast and slow components of IPSCs evoked by superficial or deep stimulation. Error bars are SE.

segregation of synaptic responses (Fig. 3), suggests that fast and slow components are generated in different parts of pyramidal cells as postulated for hippocampus. If this is true, then the observed mixture of fast and slow components in responses to both superficial and deep stimulation could be due to a limited exchange of axons between superficial and deep zones or to the spread of current over depth from stimulating electrodes. Alternatively, there could be a well-segregated innervation of two discrete groups of synapses, each of which evokes both fast and slow components but in different proportions as a consequence of a varying proportion of fast and slow receptors (or a single receptor with varying biexponential kinetics).

To distinguish between these possibilities, we examined the effect of focally applied bicuculline on fast and slow components of evoked IPSCs. If synapses have mixed fast and slow $GABA_A$ receptor populations and if there is a laminar segregation of synapses with different proportions of these receptors, one would expect to reduce fast and slow IPSC components by approximately the same proportion by focal application. The results of an individual experiment of this type in the distal dendritic region are illustrated in Fig. 6*A1;* pooled data are in Fig. 6*A2*. Application of bicuculline in layer Ia blocked more of the slow component in IPSCs evoked by superficial stimulation than it did the fast (slow reduced by 67 ± 6%, fast by 33 ± 8%; $n = 7$, $P < 0.01$; Fig. 6*A2*). This result indicates that there is at least some laminar segregation of fast and slow components, and a portion of the fast component evoked by superficial stimulation results from the spread of axons or stimulus to deeper layers outside the area affected by bicuculline. It further indicates that the actual percentage of slow component in distal dendritic IPSCs is greater than the 43% observed in responses to superficial stimulation (layer Ia in Table 1).

In contrast with results obtained by focal application of bicuculline to layer Ia, when bicuculline was applied in layer II at the recording site, the fast and slow components of IPSCs evoked from superficial and deep sites were blocked to an approximately equal extent (Fig. 6*B*). This result indicates that both slow and fast components are generated in the soma/proximal dendritic region (i.e., it rules out the possibility that the slow component in deep responses was a consequence of a spread of inhibitory axons from the somatic to the distal dendritic region). There was also no significant difference in the extent of blockade of fast and slow components when bicuculline was applied in the mid-apical dendritic region (layer Ib; Fig. 6*C*). However, the relative contribution of local synaptic properties and spread

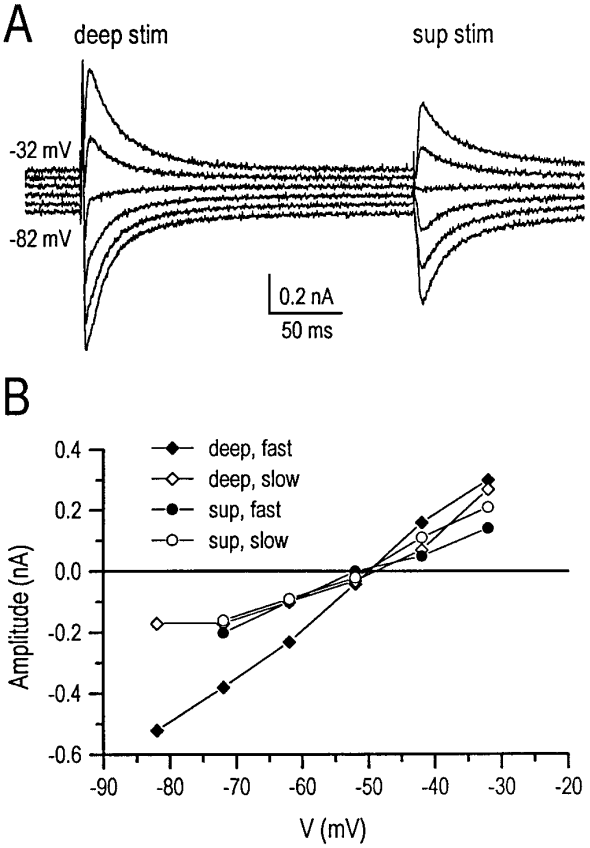


FIG. 7. Reversal potentials of fast and slow IPSC components evoked by deep and superficial stimulation were similar. *A*: IPSCs evoked by deep (layer III) and superficial (layer Ia) stimulation in a pyramidal cell at a series of holding potentials from −32 to −82 mV. *B*: reversal potentials of the fast and slow components of the superficial- and deep-evoked IPSCs were all approximately −50 mV.

of bicuculline or stimulus current cannot be distinguished in this intermediate region.

### *Reversal potentials*

Reversal potentials for the fast and slow components of IPSCs evoked from all layers were similar (Fig. 7, Table 2). The overall mean of −57 mV for IPSC reversal was ~5 mV more depolarized than the value obtained in adult rats with sharp intracellular pipettes (mean −62 mV, Table 3) (E. D. Kanter and A. Kapur, unpublished results). The younger age of the rats in the present studies (Luhmann and Prince 1991) might have contributed to a more depolarized

TABLE 2. *Reversal potentials of $GABA_A$-mediated IPSCs for slices from 3–4 wk old rats and whole cell patch pipettes*

| Stimulus Site | Component | Reversal, mV | *n* |
|---|---|---|---|
| Layer Ia | fast | −56 ± 2.9 | 9 |
| | slow | −57 ± 2.7 | 8 |
| Layer Ib | fast | −59 ± 2.5 | 8 |
| | slow | −59 ± 2.8 | 8 |
| Layer III | fast | −52 ± 2.1 | 7 |
| | slow | −53 ± 2.5 | 6 |

Values are mean ± SE.

TABLE 3. *Reversal potentials of $GABA_A$-mediated IPSCs for slices from adult rats and sharp micropipettes*

| Stimulus Site | Reversal, mV | *n* |
|---|---|---|
| Layer Ia | −62 ± 2.4 | 7 |
| Layer Ib/III | −62 ± 2 | 9 |

Values are means ± SE.

reversal potential. The substantial deviation from the value that would be predicted from the $Cl^-$ concentrations in the bathing medium and pipette solution suggests that equilibration between the contents of the relatively high resistance patch pipettes and cell bodies was incomplete. Alternatively, $HCO_3^-$ or other anions may contribute to current through $GABA_A$ channels in piriform cortex as concluded for hippo-

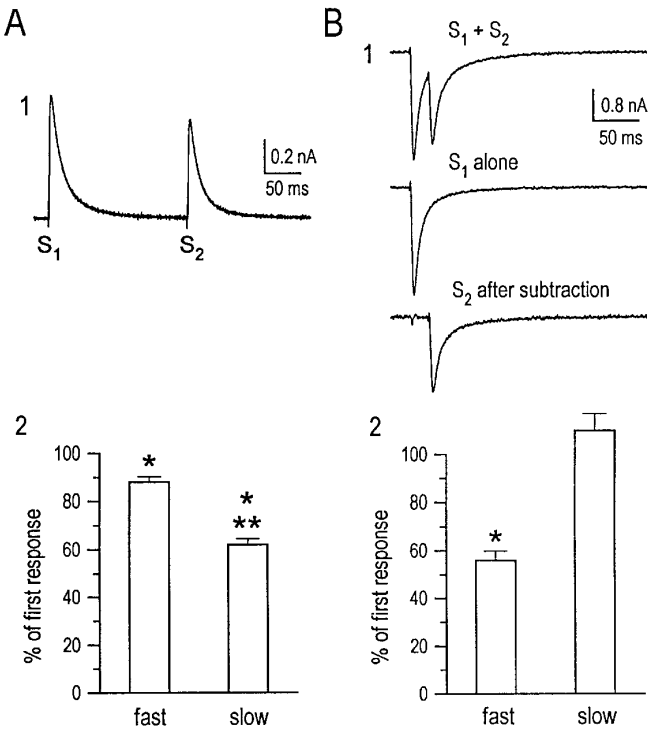


FIG. 8. Paired pulse depression of fast and slow components at long (150–200 ms) and short (10–20 ms) intershock intervals. *A*: when paired pulses were separated by 150–200 ms, the slow component of the second response was depressed more than the fast. *A1*: responses to a pair of stimuli in layer Ib separated by 200 ms. Holding potential was hyperpolarized (−67 mV) with respect to $GABA_A$ reversal so that current is inward. Coefficient of the slow component in the second response was 59% of that in the first; the coefficient of the fast in the second was 89% of the first. *A2*: pooled results for 24 cells. Mean amplitudes of the fast and slow components in the second response are expressed as a percentage of their amplitudes in the first response. Stimuli were separated by 150–200 ms. *B*: fast component was selectively depressed when paired pulses were separated by 10–20 ms. *B1*: responses to a pair of identical stimuli in layer Ib separated by 20 ms from a different cell than illustrated in *A1*. Holding potential was −30 mV. *Top*: response to the shock pair (S1,S2). *Middle*: response to first shock alone (S1). *Bottom*: after subtraction of the response to the first shock alone. Coefficient of the fast component in the second response was 59% of that in the first; the coefficient of the slow in the second was 97% of the first. *B2*: pooled data as in *A2*, but for intervals of 10–20 ms ($n$ = 9). Error bars in *A2* and *B2* are SEs. * Significantly different from 100% ($P < 0.0001$, 1 group $t$-test). ** Depression of slow component significantly greater than depression of fast ($P < 0.0001$, paired $t$-test).

campus (Bonnet and Bingmann 1995; Fatima-Shad and Barry 1993; Staley et al. 1995).

### *Use-dependent depression of $GABA_A$-mediated IPSCs*

The hypothesis that the slow $GABA_A$ component is selectively susceptible to presynaptic $GABA_B$ inhibition was tested using paired pulse depression (PPD) and pharmacological manipulation. The strength of presynaptic $GABA_B$ regulation was assessed by measuring PPD of the IPSC at an intershock interval of 150–200 ms where presynaptic $GABA_B$ inhibition is near maximal. PPD also was measured at a shorter interval (10–20 ms).

When paired shocks were separated by 150–200 ms, significant PPD of the IPSC was observed (Fig. 8*A1*). Peak amplitude of the response to the second shock was 77 ± 1% of response to the first ($n = 24$, significantly different from 100%; $P < 0.0001$, 1 group *t*-test). Comparison of fast and slow components revealed that both were depressed, but the slow component was depressed significantly more (Fig. 8*A2*). Peak amplitude of the slow component in the second response was 62 ± 2% of that in the first versus 88 ± 2% for the fast component ($n = 24$, $P < 0.0001$, paired *t*-test).

At short intervals (10–20 ms), peak amplitude of the second response also was depressed (Fig. 8*B1*). After the response to the first stimulus alone was subtracted, the peak amplitude of the second was 70 ± 2% of the first, $n = 9$, $P < 0.0001$, 1 group *t*-test). In contrast to long intervals, there was a selective depression of the fast component at short intervals (Fig. 8*B2*). Peak amplitude of the fast component in the second response was 56 ± 4% of that in the first versus 110 ± 7% for the slow ($n = 9$, $P < 0.0001$, paired *t*-test).

To determine whether PPD of IPSCs is dependent on the activation of presynaptic $GABA_B$ receptors, effects of the specific $GABA_B$ antagonist CGP 35348 were examined. At the 150- to 200-ms interval, CGP 35348 partially reversed the depression of the slow component (Fig. 9*A*). Depression of the peak amplitude decreased from 35 ± 6% to 18 ± 6%, ($n = 5$, $P < 0.0005$, paired *t*-test). The fast component was not depressed at the 150- to 200-ms interval, and CGP 35348 caused no further change ($n = 5/5$; Fig. 9*A*).

CGP 35348 also did not alter PPD of the fast component at the 10- to 20-ms interval (Fig. 9*B*). Depression of the fast component was 48 ± 6% in DNQX and APV, and 57 ± 6% after addition of CGP 35348, ($n = 3$, $P = 0.454$, paired *t*-test). Hence, the depression of the fast component at short intervals does not appear to be mediated by $GABA_B$ receptors, as expected from the slow onset of this inhibitory process.

To test for the presence of presynaptic $GABA_B$ receptors that could block the slow $GABA_A$ component, effects of the $GABA_B$ agonist baclofen were examined (Fig. 10). After bath application of R(+)-baclofen (0.5 mM), peak amplitude of the slow component was reduced to 47 ± 2% of the control level, whereas peak amplitude of the fast was 85 ± 7% of control ($n = 4$, $P < 0.025$, paired *t*-test).

Because presynaptic $GABA_B$-mediated inhibition reduces the release of GABA, the finding that this process acts selectively on the slow component suggests that fast and slow components are mediated to a large extent by different synaptic terminals.

## DISCUSSION

### *$GABA_A$-mediated IPSCs are generated in apical dendrites of pyramidal cells in piriform cortex*

The results provide the first direct evidence for the generation of $GABA_A$-mediated IPSCs in the dendrites of pyramidal cells in piriform cortex: IPSCs evoked by superficial stimulation (layer Ia) were blocked at brief delays after the application of bicuculline to distal segments of apical dendrites in contrast to a long delay and lesser extent with application near cell bodies. A previous study had provided indirect evidence for dendritic $GABA_A$-mediated inhibition through the demonstration that dendritic, but not somatic, application of bicuculline facilitates the NMDA component of EPSPs in dendrites (Kanter et al. 1996).

There is much evidence for the hippocampus and neocortex that $GABA_A$-mediated inhibition also is generated in the dendrites of pyramidal cells. In the CA1 region of hippocampus, studies with combined anatomy and physiology (Buhl et al. 1994a; Miles et al. 1996), current source-density analysis (Lambert et al. 1991) and local application of bicuculline (Pearce 1993), indicate that $GABA_A$-mediated IPSCs are generated in both apical and basal dendrites of pyramidal cells. In cat motor cortex, evidence has been provided that inhibitory neurons in all layers give rise to horizontal axons that generate $GABA_A$-mediated IPSPs in apical dendrites of pyramidal cells (Kang et al. 1994). It therefore appears that dendritic $GABA_A$-mediated inhibition is a general feature of pyramidal cells in cerebral cortex.

### *Inhibition in piriform cortex is segregated in depth and mediated by feedforward and feedback pathways*

The results obtained by stimulation in different layers and application of bicuculline at different locations on pyramidal cells (Fig. 3) indicate that different populations of GABAergic interneurons provide input to distal dendritic and somatic regions of pyramidal cells. If axonal processes from superficial and deep populations were to overlap extensively, the observed laminar specificity in the action of bicuculline could not have been obtained. Preliminary results obtained by intracellular dye injection of interneurons in piriform cortex support this conclusion (Ekstrand and Haberly 1995; Ekstrand et al. 1996). For the hippocampus, there is an extensive literature supporting such laminar specificity in inhibitory circuitry that includes studies combining anatomic and physiological methods (Buhl et al. 1994a,b, 1995; Freund and Buzaki 1996; Halasy and Somogyi 1993; Lacaille et al. 1989; Miles et al. 1996).

Because the termination of afferent fibers is confined to layer Ia in piriform cortex (Price 1973), the present evidence for GABAergic neurons and axons in this layer suggests that afferents mediate a feedforward inhibition onto the apical dendrites of pyramidal cells (see Fig. 1). Studies in progress have shown that interneurons in layer Ia are excited by afferent fibers, consistent with this hypothesis (Ekstrand and Haberly 1995).

Because the association fibers in layers Ib, II, and III are recurrent axon collaterals from pyramidal cells, GABAergic neurons in these layers are candidates for the mediation of feedback inhibition onto pyramidal cells (see Fig. 1). Previ-

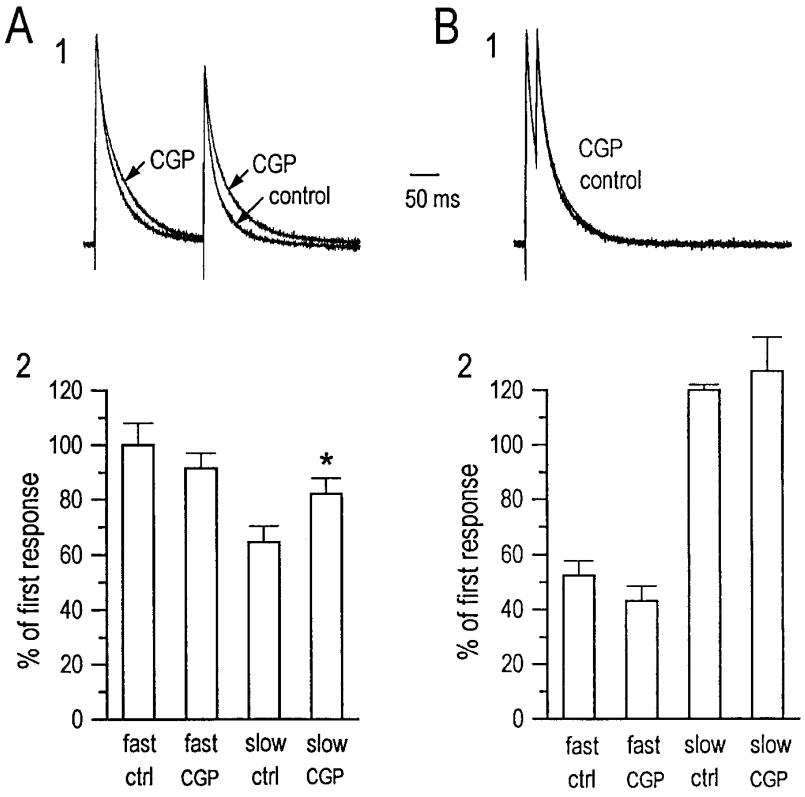


FIG. 9. The $GABA_B$ antagonist 3-amino-propyl (diethoxymethyl) phosphinic acid 35348 (CGP) reduced paired pulse depression (PPD) at long, but not short intervals. *A*: paired pulses at long intervals. *A1*: sample responses to paired stimulation in layer Ia before and after bath application of 1 mM CGP, 200-ms interval. Peaks of the first responses are normalized. *A2*: pooled data for long interval. Mean amplitudes of fast and slow components in the second response are expressed as a percentage of the first response amplitudes before (ctrl) and after CGP. Note that CGP partially reversed the depression of the slow component. * Difference between control and CGP conditions significant at $P < 0.005$ (paired *t*-test). *B*: paired pulses at brief intervals. *B1*: sample responses to paired stimulation in layer Ib before and after CGP, same cell as in *A1* but pulses separated by 20 ms. Peaks of first responses are normalized. *B2*: pooled data as in *A2*, except for 10- to 20-ms intervals. Error bars in *A2* and *B2* are SEs.

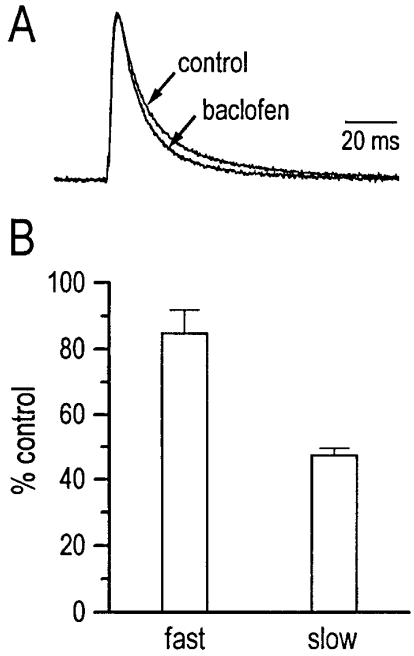


FIG. 10. R(+)-baclofen preferentially reduced the slow component of the $GABA_A$-mediated IPSC. *A*: $GABA_A$-mediated IPSC evoked from layer Ib before (control) and after bath application of 0.5 $\mu$M R(+)-baclofen. Peaks have been normalized to illustrate differences in their time courses. Coefficient of the slow component in baclofen was 45% of that in the control; coefficient of the fast component in baclofen was 84% of control. *B*: pooled data. Mean amplitudes of fast and slow components in baclofen expressed as a percentage of their control amplitudes. Error bars are SEs.

ous studies with a variety of anatomic and physiological methods have provided evidence for the presence of such feedback circuitry in piriform cortex (Biedenbach and Stevens 1969; Gellman and Aghajanian 1993; Haberly and Bower 1984; Kubota and Jones 1992; Satou et al. 1983). The present studies provide additional evidence that the action of this circuitry is concentrated in somatic and proximal dendritic regions of pyramidal cells.

### *$GABA_A$-mediated IPSCs in piriform cortex have fast and slow components*

The results suggest that two kinetically distinct $GABA_A$-mediated IPSC components are present in pyramidal neurons in piriform cortex: a fast component that decays with a time constant of 6–15 ms and a slow component with a decay time constant of 30–80 ms. Several lines of evidence suggest that the slow component represents a longer lasting conductance rather than a space-clamp artifact. First, the delayed voltage-step experiment (Fig. 5) indicates that capacitative current is not responsible for the slow decay. Second, the evidence that both fast and slow components are generated in distal dendrites and in the vicinity of cell bodies (Figs. 4 and 6) is incompatible with an artifactual origin of the slow component from an inadequate space clamp. Third, reduction in the extent of PPD of the slow but not the fast IPSC component by CGP 35348 and a greater block of the slow component by baclofen suggests that the two are generated by different populations of synaptic terminals. A dissociation in the effect of baclofen on fast and slow components also has been reported in the hippocampal CA3 (Lambert and Wilson 1993) and CA1 (Pearce et al. 1995) regions. Finally,

in a computer simulation analysis (APPENDIX A), the observed slow component could not be replicated with fast-only $GABA_A$ conductances on dendrites. In contrast, the observed IPSCs could be simulated readily with a mixture of fast and slow $GABA_A$ conductances (APPENDIX B).

Time constants of the fast and slow components recorded in the hippocampus were 3–8 and 30–70 ms, respectively (Pearce 1993). In the present study, the fast time constant ranged from 6 to 15 ms and the slow from 30 to 80 ms, consistent with the lower recording temperature (29 vs. 36°C). $GABA_A$-mediated IPSCs with dual decay time constants of $7 \pm 1.6$ ms and $59 \pm 16$ ms at 22–24°C also have been reported in cerebellar granule cells (Puia et al. 1994).

### *Fast and slow $GABA_A$ conductances are differentially distributed in somatic and distal dendritic regions*

The results obtained by focal application of bicuculline suggest that both fast and slow $GABA_A$ components are generated in somatic and dendritic regions of pyramidal cells but that the distribution of the slow component is skewed toward the distal dendritic region and the fast skewed toward the somatic region. However, the simulation studies presented in APPENDIX B reveal that the present evidence cannot exclude the possibility that cell bodies express only the fast component and that distal-most apical dendrites express only the slow.

### *Use-dependent depression of fast and slow components of $GABA_A$-mediated IPSCs*

The susceptibility of $GABA_A$ mediated IPSCs to depression during repetitive activation was assessed by examining the extent of PPD. These studies revealed that $GABA_A$-mediated IPSCs are depressed at both long (150–200 ms) and short (10–20 ms) intervals. At long intervals, the slow component was depressed preferentially, whereas at short intervals only the fast component was depressed. A similar result was obtained in the hippocampal CA1 region (Pearce et al. 1995) where paired-pulses with intervals of 150–200 ms depressed the slow component by ~50% but did not reduce the fast component, whereas paired-pulses with intervals of 20–40 ms depressed the fast component by ~30% but did not affect the slow component. It is interesting to note that a commonly used LTP-inducing protocol, theta-burst stimulation (Larson and Lynch 1988), uses both long and short intervals as tested above and therefore would result in the depression of both the slow and fast $GABA_A$-mediated IPSCs, but depression of the slow would develop more slowly and be much longer lasting.

Results with a specific antagonist provided evidence that the slow component, but not the fast, is regulated by $GABA_B$ receptors. This finding supports a role for the slow $GABA_A$ component in the regulation of the NMDA-dependent LTP as discussed below.

Simulations presented in APPENDIX C indicate that the extent of PPD of the fast component at 10- to 20-ms intervals was overestimated as a consequence of the somatic recording of dendritic conductances. The resulting incomplete control of voltage at the generation site would reduce the driving force during the peak of the second response thereby decreasing the amplitude of the recorded current.

### *Functional implications*

The results are consistent with a role of dendritic $GABA_A$-mediated inhibition in the regulation of NMDA-mediated processes in piriform cortex. Such regulation would have an impact on the integration of repetitive inputs that can activate the NMDA component as well as on NMDA-dependent LTP (Artola et al. 1990; Kanter and Haberly 1993; Steward et al. 1990; Wigström and Gustafsson 1983). The laminar specificity in inhibitory circuitry that has been demonstrated could allow a relatively selective block of the dendritic $GABA_A$-mediated IPSC by action of centrifugal inputs or local processes at the interneuronal level. In the companion paper, evidence will be presented that the greater proportion of the slow $GABA_A$ component in distal apical dendrites on which afferent fibers synapse could increase the efficacy of this control: computer simulation studies confirmed that the slow component is more effective that the fast for control of current through NMDA channels and the resulting depolarization (Kapur et al. 1997). Regulation of the slow component by presynaptic $GABA_B$ receptors further supports a role of this process in the control of NMDA-dependent synaptic plasticity, because, in the hippocampus, a reduction in strength of $GABA_A$-mediated inhibition by presynaptic $GABA_B$ regulation is required for the induction of LTP (Davies et al. 1991; Mott and Lewis 1991). This requirement, together with a lack of presynaptic $GABA_B$ inhibition of the fast $GABA_A$ component, indicates that regulation of NMDA-dependent LTP by GABAergic inhibition in hippocampus is exclusively by way of the slow component (Pearce et al. 1995).

Dendritic $GABA_A$-mediated IPSCs also would be expected to influence $Na^+$ and $Ca^{2+}$ channels in dendrites (Gillessen and Alzheimer 1997; Lipowsky et al. 1996; Magee and Johnson 1995; Schwindt and Crill 1995), one action of which is presumably a modulation of the NMDA component. Regulation of voltage-gated $Ca^{2+}$ channels by dendritic $GABA_A$-mediated inhibition also might play a role in control of NMDA-independent synaptic plasticity (Johnston et al. 1992). The ability of dendritic $GABA_A$-mediated inhibition to block burst firing mediated by dendritic $Ca^{2+}$ channels in pyramidal cells in the CA3 region of hippocampus supports this role (Miles et al. 1996; Traub et al. 1994). Dendritic GABAergic inhibition also would modulate the back-propagation of $Na^+$ spikes into dendrites from cell bodies (Magee and Johnston 1997; Svoboda et al. 1997; Tsubokawa and Ross 1996). Because NMDA-dependent LTP of weak EPSPs can be enabled by a pairing with back-propagating action potentials (Magee and Johnston 1997; Markram et al. 1997), this could provide an additional means for GABAergic regulation of synaptic plasticity.

In addition to regulating integrative processes and synaptic plasticity, inhibitory processes must maintain local and system-wide excitability in a range that allows normal function but avoids pathological bursting. The potential for such bursting is present in most areas of cerebral cortex including piriform cortex as a consequence of extensive positive feedback circuitry. The changing needs of different functional states with associated differences in activity level and many other factors makes this a formidable task. The relative independence in inhibitory circuits that impinge on somatic and

dendritic regions would appear to be a specialization that assists in this role. The significance of this independence is further examined with modeling methods in the companion paper (Kapur et al. 1997).

## APPENDIX A

### *Can the biexponential decay of $GABA_A$-mediated IPSCs be reproduced with monoexponentially decaying dendritic inputs?*

Because the true time course of synaptic processes in dendrites is faster than the time course recorded in voltage-clamp mode from the cell body, the possibility must be considered that the observed biexponential decay in $GABA_A$-mediated IPSCs is artifactual. To explore this possibility, simulations were carried out with the model cell described in the companion paper (Kapur et al. 1997). This model was developed from a serially reconstructed layer II pyramidal cell in piriform cortex with physiological data derived by whole cell patch recording. The morphologically complete version of the model (345 compartments) was used for all simulations. The conductance change associated with the activation of $GABA_A$ synaptic inputs ($GABA_A$ conductance) was simulated with exponential rising and falling phases as follows

$$G_A = \bar{g}_f(1 - e^{-t/\tau_r})e^{-t/\tau_d}$$

where $G_A$ = $GABA_A$ conductance, $\bar{g}_f$ = maximum conductance, $\tau_r$ = time constant of rising phase, and $\tau_d$ = time constant of decay.

CASE 1: FAST $GABA_A$ CONDUCTANCES ON DISTAL APICAL DENDRITES. The objective was to match a typical somatic voltage-clamp response evoked by superficial stimulation (layer Ia) in a slice in which $GABA_A$-mediated IPSCs were pharmacologically isolated (Fig. 4*A*).

The time constant of decay for the fast $GABA_A$ conductance was assumed to be 10 ms (Table 1). Two hundred of these $GABA_A$ conductances were placed on the distal portion of the apical dendrite of the model cell starting at 325 $\mu$m from the cell body. The cell body was clamped at −35 mV (level in most of the present experiments) during application of the $GABA_A$ conductance. Runs were performed with two values of $R_i$ (100 and 200 $\Omega$cm) and two values of $R_m$ (26,845 and 67,114 $\Omega cm^2$) that yielded membrane time constants of 40 and 100 ms, respectively, with $C_m$ = 1.49 $\mu F/cm^2$ (the computed value for the modeled cell). The response was a simulated somatic voltage-clamp recording (current required at the cell body to maintain a constant potential at this location during activation of the dendritic conductances). The results revealed a substantial slowing of the decay phase of the somatic current relative to the time course of the applied $GABA_A$ conductance, as expected (Fig. A1*A*). However, convergence could not be obtained with a biexponential fit with any combination of parameters, and the time constants for monoexponential fits were 23–30 ms in contrast to experimentally derived values for the slow $GABA_A$ component of 30–80 ms.

CASE 2: FAST $GABA_A$ CONDUCTANCES ON PROXIMAL AND DISTAL APICAL DENDRITES. Because the observed biexponential decay could not be reproduced with a monoexponentially decaying conductance on distal dendritic segments, a second series of simulations was carried out with two populations of $GABA_A$ conductances at different distances from the cell body. The maximal conductances for the two populations were varied in an attempt to reproduce the observed biexponential decay. The rationale for this exploration was that a distal population could reproduce the slow component and a more proximal population could reproduce the fast. The distal population consisted of 100 synapses that were distributed randomly over compartments at 300–600 $\mu$m from the cell body, and the proximal population, 100 synapses randomly distributed at 75–300 $\mu$m from the cell body (the proximal distribution stopped short of the cell body because somatic application of bicuculline had little effect on superficial-evoked IPSCs). Sensitivity to relevant parameters was examined as follows:

*1*) The time constant of decay ($\tau_d$) for the $GABA_A$ conductance was varied from 7 to 10 ms in steps of 1 ms. Tests showed that simulated somatic IPSC recordings with a slow component in the experimentally observed range (>30 ms) could not be reproduced when $\tau_d$ was <7 ms.

*2*) Maximum conductance of proximal $GABA_A$ synapses was varied from 1 to 2 nS in steps of 0.25 nS. Tests showed that

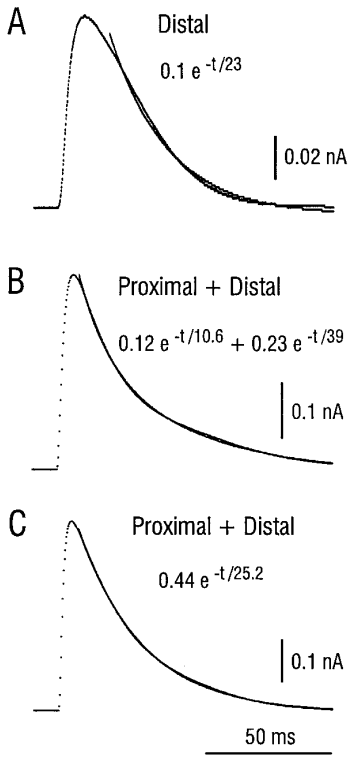


FIG. A1. Simulated somatic voltage-clamp recordings of dendritic $GABA_A$-mediated IPSCs. Simulations were carried out with the compartmental model of a layer II pyramidal cell (*40C2*) developed in the companion paper (Kapur et al. 1997). *A*: with fast-only $GABA_A$ conductances confined to distal apical dendrites, response decays could not be well-fitted with either mono- or biexponential functions. Illustrated trace was obtained with 200 conductances with a decay time constant ($\tau_d$) = 10 ms and maximum conductance ($\bar{g}$) = 0.5 nS at distances ≥ 325 $\mu$m from the cell body. Closest fit was the illustrated single exponential with a time constant of 23 ms. *B*: when fast-only $GABA_A$ conductances were distributed over middle and distal apical segments, decay of the somatic response could be biexponential. Illustrated result (best match to actual response) was obtained with 100 conductances with $\tau_d$ = 10 ms and $\bar{g}$ = l50 nS on distal segments at 300–600 $\mu$m from the cell body, and 100 conductances with $\tau_d$ = 10 ms and $\bar{g}$ = 2 nS on middle apical segments at 75–300 $\mu$m from the cell body. Slow time constant for the biexponential fit (39 ms) was at the lower limit of actual responses (48 ± 3 ms), as was the contribution of the fast component to peak amplitude (34% vs. 57 ± 4%). *C*: fast-only conductances on middle and distal segments also could generate a monoexponential decay. Illustrated result was obtained with 100 conductances with $\tau_d$ = 10 ms and $\bar{g}$ = 17.5 nS at 300–600 $\mu$m from the cell body and l00 with $\tau_d$ = 10 ms and $\bar{g}$ = 1.75 nS at distances of 75–300 $\mu$m. In all simulations (*A–C*), reversal potential of the leak conductance was −50 mV (approximate value with $Cs^+$-containing patch pipettes); holding potential at the cell body was −35 mV. Passive membrane constants were: $R_m$ = 26,845 $\Omega cm^2$ and $C_m$ = 1.49 $\mu F/cm^2$ for *A–C*; $R_i$ = 200 $\Omega$cm in *A* and *C* and 300 $\Omega$cm in *B*.

maximum values <1 nS gave a negligible fast component in simulated IPSC recordings.

*3*) Maximum conductance of distal $GABA_A$ synapses was 10, 25, or 40 times the maximum conductance of the proximal population. Tests showed that when maximum conductance for the distal population was <10 times that of the proximal, an adequate slow component could not be obtained.

*4*) $R_i$ was varied from 100 to 400 Ωcm in steps of 100 Ωcm.

*5*) Two sets of values for $C_m$ and $R_m$ were tested that yielded membrane time constants ($\tau_m$) in the range observed experimentally with $Cs^+$-containing patch pipettes. $C_m = 2\ \mu F/cm^2$ and $R_m = 26{,}845\ \Omega cm^2$ yielded a $\tau_m = 40$ ms; $C_m = 1.5\ \mu F/cm^2$ and $R_m = 50{,}000\ \Omega cm^2$ yielded $\tau_m = 100$ ms. The reversal potential of the leak conductance (represented by $R_m$) was set to −50 mV, again to reproduce findings with $Cs^+$-containing pipettes in slices from immature animals.

For each combination of parameters, two randomly chosen synaptic distributions were used to ensure insensitivity to the exact placement of synapses. For each of 960 runs, an attempt was made to fit the decay phase of the simulated somatic IPSC recording with a biexponential function. If the fitting routine failed to converge, a monoexponential fit was attempted. Sample responses with biexponential and monoexponential fits are illustrated in Fig. A1, *B* and *C*. To determine whether the simulated IPSCs were comparable with the experimentally recorded IPSCs, the following criteria were employed:

*1*) A decay phase that could be fitted well with a biexponential function, with the amplitude of each component comprising ≥20% of the peak amplitude.

*2*) A fast component with a time constant between 6 and 15 ms.

*3*) A slow component with a time constant between 30 and 80 ms.

*4*) A ratio of slow to fast components ($\tau_s$:$\tau_f$) >3.5. Experimentally, $\tau_s$:$\tau_f = 4.61 \pm 0.28$ (Table 1).

Although a number of combinations of parameters were found that satisfied these criteria (● in Fig. A2), the proportion of the fast component was, at best, at the lower limit of the experimentally observed range (maximum of 35% vs. 57 ± 4% for actual responses, Table 1).

A search for simulated IPSCs that satisfied criteria 1–3, with the additional constraint of a contribution of the fast component >40%, also resulted in several successful combinations (○ in Fig. A2). However, maximum $\tau_s$:$\tau_f$ was 3.4 versus 4.61 ± 0.28, as observed experimentally (Table 1).

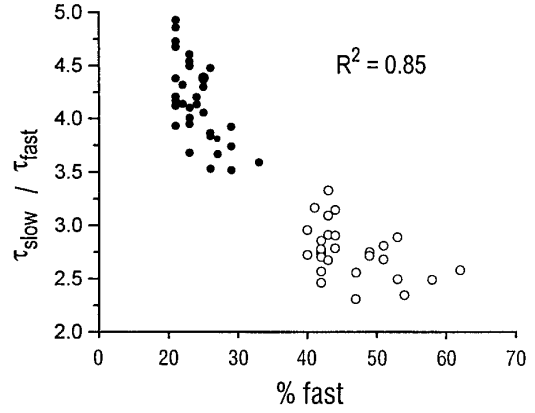


FIG. A2. Simulated somatic voltage-clamp recordings of dendritic $GABA_A$ IPSCs with fast-only decays do not match experimentally recorded IPSCs. Each point is a result from a systematic parameter exploration for which the decay phase could be well fit by a biexponential function with a fast time constant ($\tau_f$) between 6 and 15 ms and a slow time constant ($\tau_s$) between 30 and 80 ms. Results of 2 explorations are presented: ●, results for which $\tau_s$:$\tau_f$ was within the experimental range; ○, results for which the percent contribution of the fast component to peak amplitude was within the experimental range. As described in the text, when $\tau_s$:$\tau_f$ was in-range, percent fast was not, and when percent fast was in-range, $\tau_s$:$\tau_f$ was not.

In four cases in which $\tau_s$:$\tau_f$ exceeded 3.5, the simulations were repeated with the proximal population of $GABA_A$ conductances starting at 25 μm from the cell body rather than 75 μm, in an attempt to increase the proportion of the fast component. This resulted in a maximum contribution of the fast component of 42%—still at the lower limit of the experimentally observed values.

In summary, with a monoexponentially decaying $GABA_A$ conductance, the experimental IPSC recorded at the cell body, which has a large fast component and a high $\tau_s$:$\tau_f$ ratio, could not be duplicated. In cases where a monoexponential fit was better than a biexponential, the slowest time constant was 30 ms, which was substantially faster than the time constant of the actual slow component evoked by superficial stimulation (Table 1). It therefore is concluded that the experimentally observed biexponential decay results from the presence of fast and slow $GABA_A$ conductance components.

## APPENDIX B

### *Simulation of biexponential IPSCs with fast and slow $GABA_A$ conductances*

Based on the failure of simulations with a single time constant of decay to adequately reproduce the observed IPSCs, studies were carried out with the assumption that there are two $GABA_A$ conductance components with fast and slow time constants of decay that are distributed differentially on the apical dendrite. These simulations were carried out with the same model cell used for the studies in APPENDIX A, with the cable parameters that provided the best fit to voltage transients for the modeled cell [$R_i = 137\ \Omega cm$, $R_m = 14{,}005\ \Omega cm^2$, and $C_m = 1.49\ \mu F/cm^2$; *cell 40C2* in Table 1 from Kapur et al. (1997)] and a resting potential (reversal for $R_m$) of −50 mV.

The distribution of GABAergic synapses on pyramidal cells in rat piriform cortex is unknown, but numbers are available for the opossum piriform cortex (L. B. Haberly and S. L. Feig, unpublished results), which closely resembles rat piriform cortex both morphologically and physiologically. The values for the opossum were derived with the method of Cruz-Orive (1977) that was validated by direct counts in serial sections. Synapses with symmetrical contacts and associated pleomorphic vesicles were assumed to be GABAergic. Calculations were made of the number per unit volume as a function of depth within layer I. Because this layer contains few dendrites of nonpyramidal cells (Haberly 1983; Haberly and Feig 1983), these numbers are thought to be reasonable estimates for synaptic inputs to pyramidal cell dendrites. The same methods were used to estimate the number of synapses with round vesicles and asymmetrical contacts (presumed glutamatergic synapses). Because dendritic spines on pyramidal cells in piriform cortex typically receive a single synapse of this form, these estimates are approximately equal to the volume density of spines. From the ratio of the volume density of spines to the volume density of putative GABAergic synapses for the opossum and from the present estimates of spines per unit membrane area for the rat (Kapur et al. 1997), estimates of the density of GABAergic synapses per unit membrane area were derived for different dendritic segments (Tables 2 and 3 in Kapur et al. 1997). Dendritic compartments of the model cell were chosen for the assignment of GABAergic synapses by random sampling using the estimates in Table 2 from Kapur et al. (1977) and the locations and dimensions of compartments in the model cell.

To replicate IPSCs evoked by superficial stimulation, 100 fast

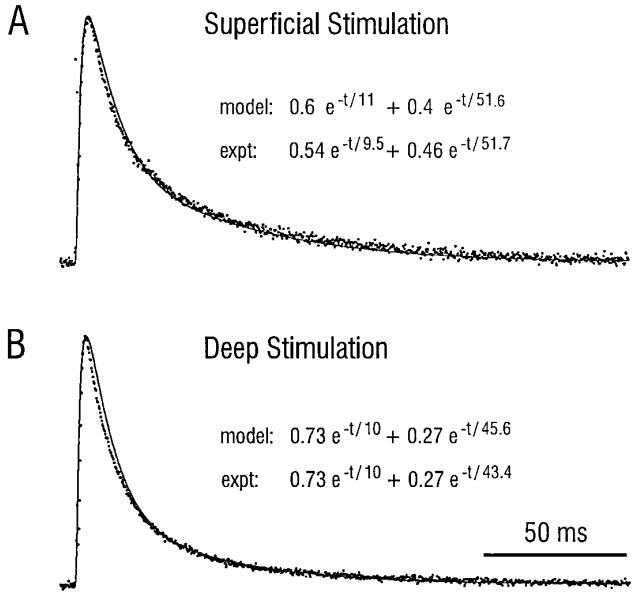


FIG. B1. IPSCs simulated by a combination of fast and slow $GABA_A$ components in apical dendrites can match experimentally recorded IPSCs. *A*: experimental IPSC evoked by superficial stimulation (●) and simulated IPSC (——). Both time constants and relative proportions of the 2 components were well reproduced by the model. *B*: same as *A* but for deep stimulation.

and 100 slow $GABA_A$ conductances were placed at different locations on the apical dendrite. Fast conductances with $\tau_d = 7.25$ ms and $\bar{g} = 1.15$ nS were distributed randomly in apical dendritic compartments at 100–400 $\mu$m from the cell body. Slow conductances with $\tau_d = 37$ ms and $\bar{g} = 0.25$ nS were placed on compartments at 200–600 $\mu$m from the cell body. These distributions were loosely based on the experimental observations that both fast and slow components of the IPSC evoked by superficial stimulation were blocked by bicuculline in the mid-apical dendritic region (Fig. 6*C*) and that the slow component was blocked to a greater extent in the distal apical region (Fig. 6*A*). No GABAergic inputs were placed on the soma or basal dendrites because local application of bicuculline at the depths of these structures had little effect on the response to superficial stimulation. This distribution of conductances produced simulated IPSCs that adequately matched actual IPSCs evoked by superficial stimulation: decay time constants were 11 and 51.6 ms, and the fast component constituted 60% of the peak amplitude (Fig. B1*A*).

To replicate IPSCs evoked from deep stimulation (association fiber layers), 100 slow GABAergic conductances ($\tau_d = 37$ ms, $\bar{g} = 0.2$ nS) were distributed on apical and basal dendrites at distances of 100–300 $\mu$m from the cell body. Ninety out of a total of 100 fast $GABA_A$ conductances ($\tau_d = 7.25$ ms, $\bar{g} = 1.0$ nS) were placed on apical and basal dendrites at distances of 0–300 $\mu$m from the soma; the remaining 10 were placed on the cell body. This distribution of fast and slow conductances produced a realistic IPSC at the soma that decayed biexponentially with time constants of 10 and 45.6 ms, with the fast component comprising 73% of the peak amplitude (Fig. B1*B*).

Several conclusions can be drawn from these simulations: First, the experimentally observed biexponentially decaying IPSCs can be reproduced readily with fast and slow $GABA_A$ components. Second, true fast and slow time constants are somewhat faster than those derived experimentally. Third, the results suggest that both fast and slow components are present in $GABA_A$-mediated IPSCs in middle as well as distal apical dendritic segments. In the experimental studies, it was not possible to make this determination for the mid-apical dendritic region because of uncertainties about the extent of spread of locally applied bicuculline. Finally, the simulations show that the observed results can be replicated with IPSCs with exclusively fast $GABA_A$ conductances on cell bodies.

## APPENDIX C

### *Extent of artifactual PPD of the IPSC from imperfect voltage clamp*

In response to the second of a pair of stimulus pulses separated by a brief (10–20 ms) interval, the fast-decaying component of the $GABA_A$-mediated response was depressed significantly. A potential problem in interpretation is that an imperfect voltage clamp could produce a similar decrease in amplitude. This is because the driving force for the IPSC would be decreased during the response to the second stimulus if voltage is not well controlled during the response to the first. Because the extent of this error would decrease over time, it would be greatest for the fast component at short intershock intervals. To evaluate the extent of this error, simulations were carried out with the same parameters used to replicate the deep stimulus-evoked IPSC in APPENDIX B. The simulated response to paired activation of identical conductances separated by 10 ms is illustrated in Fig. C1*A*. Comparison of the response to the first stimulus alone (Fig. C1*B*) with the subtraction-isolated response to the second stimulus of the pair (Fig. C1*C*) reveals a decrease in amplitude as a result of the incomplete dendritic voltage clamp. The fast component was decreased by 22%, which compares with a typical 50% decrease observed experimentally (Fig. 8). It is concluded that there is a PPD of the fast $GABA_A$ component at short intervals, but the magnitude of depression is approximately one-half that observed experimentally in somatic voltage-clamp recordings.

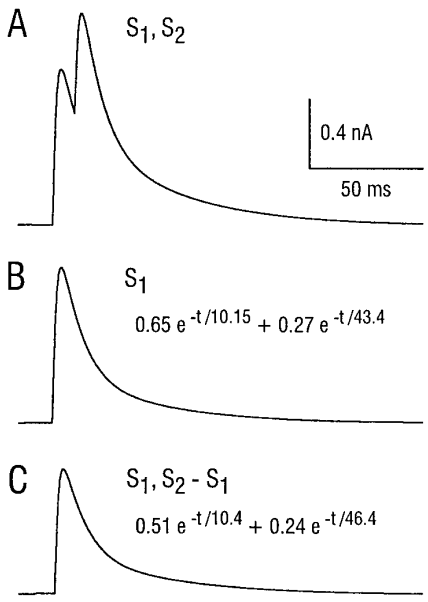


FIG. C1. Evaluation of the extent of artifactual paired pulse depression of dendritic $GABA_A$-mediated IPSCs when voltage clamp is applied at the cell body. *A*: simulated somatic recording of identical IPSCs separated by 10 ms. *B*: simulated recording of first IPSC alone. *C*: simulated recording of the second IPSC in the pair, isolated by subtracting the response in *B* from that in *A*. Peak amplitude of the isolated second response was 81% of the first. Fast component was depressed by 22% and the slow by 11%. Passive membrane properties and synaptic distributions used for the simulation were the same as those for Fig. B1*B*.

We thank M. Hines for technical assistance with Neuron.

This work was supported by National Institute of Neurological Disorders and Stroke Grant NS-19865 to L. B. Haberly.

Present address of A. Kapur: Div. of Neuroscience, Baylor College of Medicine, Houston, TX 77030.

Address for reprint requests: L. B. Haberly, Dept. of Anatomy, University of Wisconsin, 1300 University Ave., Madison, WI 53706.

Received 19 March 1997; accepted in final form 3 July 1997.

## REFERENCES

ARTOLA, A., BROCHER, S., AND SINGER, W. Different voltage-dependent thresholds for inducing long-term depression and long-term potentiation in slices of rat visual cortex. *Nature* 347: 69–72, 1990.

BIEDENBACH, M. A. AND STEVENS, C. F. Synaptic organization of the cat olfactory cortex as revealed by intracellular recording. *J. Neurophysiol.* 32: 204–214, 1969.

BLANTON, M. G., LO TURCO, J. J., AND KRIEGSTEIN, A. R. Whole cell recording from neurons in slices of reptilian and mammalian cerebral cortex. *J. Neurosci. Methods* 30: 203–210, 1989.

BONNET, U. AND BINGMANN, D. $GABA_A$-responses of CA3 neurones: contribution of bicarbonate and of $Cl^-$-extrusion mechanisms. *Neuroreport* 6: 700–704, 1995.

BUHL, E. H., COBB, S. R., HALASY, K., AND SOMOGYI, P. Properties of unitary IPSPs evoked by anatomically identified basket cells in the rat hippocampus. *Eur. J. Neurosci.* 7: 1989–2004, 1995.

BUHL, E. H., HALASY, K., AND SOMOGYI, P. Diverse sources of hippocampal unitary inhibitory postsynaptic potentials and the number of synaptic release sites. *Nature* 368: 823–828, 1994a.

BUHL, E. H., HAN, Z.-S., LORINCZI, A., STEZHKA, V. V., KARNUP, S. V., AND SOMOGYI, P. Physiological properties of anatomically identified axo-axonic cells in the rat hippocampus. *J. Neurophysiol.* 71: 1289–1307, 1994b.

CRUZ-ORIVE, L.-M. Particle size-shape distributions: the general spheroid problem. *J. Morphol.* 112: 153–167, 1977.

DAVIES, C. H., STARKEY, S. J., POZZA, M. F., AND COLLINGRIDGE, G. L. $GABA_B$ autoreceptors regulate the induction of LTP. *Nature* 349: 609–611, 1991.

DEL CERRO, S., JUNG, M., AND LYNCH, G. Benzodiazepines block long-term potentiation in slices of hippocampus and piriform cortex. *Neuroscience* 49: 1–6, 1992.

EKSTRAND, J. J. AND HABERLY, L. B. GABAergic neurons in the molecular layer of piriform (olfactory) cortex have lamina-specific axonal arbors. *Soc. Neurosci. Abstr.* 21: 1186, 1995.

EKSTRAND, J. J., JOHNSON, D.M.G., FEIG, S. L., AND HABERLY, L. B. Cajal-Retzius-like cells in anterior piriform cortex mediate fast feedforward inhibition in a large area of the piriform cortex. *Soc. Neurosci. Abstr.* 22: 1824, 1996.

FATIMA-SHAD, K. AND BARRY, P. H. Anion permeation in GABA- and glycine-gated channels of mammalian cultured hippocampal neurons. *Proc. R. Soc. Lond. B Biol. Sci.* 253: 69–75, 1993.

FREUND, T. F. AND BUZAKI, G. Interneurons of the hippocampus. *Hippocampus* 6: 347–470, 1996.

GELLMAN, R. L. AND AGHAJANIAN, G. K. Pyramidal cells in piriform cortex receive a convergence of inputs from monoamine activated GABAergic interneurons. *Brain Res.* 600: 63–73, 1993.

GILLESSEN, T. AND ALZHEIMER, C. Amplification of EPSPs by low $Ni^{2+}$ and amiloride-sensitive $Ca^{2+}$ channels in apical dendrites of rat CA1 pyramidal neurons. *J. Neurophysiol.* 77: 1639–1643, 1997.

HABERLY, L. B. Unitary analysis of opossum prepyriform cortex. *J. Neurophysiol.* 36: 762–774, 1973.

HABERLY, L. B. Structure of the piriform cortex of the opossum. I. Description of neuron types with Golgi methods. *J. Comp. Neurol.* 213: 163–187, 1983.

HABERLY, L. B. AND BOWER, J. M. Analysis of association fiber system in piriform cortex with intracellular recording and staining methods. *J. Neurophysiol.* 51: 90–112, 1984.

HABERLY, L. B. AND FEIG, S. Structure of the piriform cortex of the opossum. II. Fine structure of cell bodies and neuropil. *J. Comp. Neurol.* 216: 69–88, 1983.

HALASY, K. AND SOMOGYI, P. Subdivisions in the multiple GABAergic innervation of granule cells in the dentate gyrus of the rat hippocampus. *Eur. J. Neurosci.* 5: 411–429, 1993.

JOHNSTON, D., WILLIAMS, W., JAFFE, D., AND GRAY, R. NMDA-receptor-independent long-term potentiation. *Annu. Rev. Physiol.* 54: 489–505, 1992.

KANG, Y., KANEKO, T., OHISHI, H., ENDO, K., AND ARAKI, T. Spatiotemporally differential inhibition of pyramidal cells in the cat motor cortex. *J. Neurophysiol.* 71: 280–293, 1994.

KANTER, E. D. AND HABERLY, L. B. Associative long-term potentiation in piriform cortex slices requires $GABA_A$ blockade. *J. Neurosci.* 13: 2477–2482, 1993.

KANTER, E. D., KAPUR, A., AND HABERLY, L. B. A dendritic $GABA_A$-mediated IPSP regulates facilitation of NMDA-mediated responses to burst stimulation in piriform cortex. *J. Neurosci.* 16: 307–312, 1996.

KAPUR, A., LYTTON, W. W., KETCHUM, K. L., AND HABERLY, L. B. Regulation of the NMDA component of EPSPs by different components of postsynaptic GABAergic inhibition: a computer simulation analysis in piriform cortex. *J. Neurophysiol.* 78: 2546–2559, 1997.

KUBOTA, Y. AND JONES, E. G. Co-localization of two calcium binding proteins in GABA cell of rat piriform cortex. *Brain Res.* 600: 339–344, 1992.

LACAILLE, J. C., KUNKEL, D. D., AND SCHWARTZKROIN, P. A. Electrophysiological and morphological characterization of hippocampal interneurons. In: *The Hippocampus–New Vistas*, edited by V. Chan-Palay and C. Kohler. New York: Liss, 1989, p. 287–305.

LAMBERT, N. A., BORRONI, A. M., GROVER, L. M., AND TEYLER, T. J. Hyperpolarizing and depolarizing $GABA_A$ receptor-mediated dendritic inhibition in area CA1 of the rat hippocampus. *J. Neurophysiol.* 66: 1538–1548, 1991.

LAMBERT, N. A. AND WILSON, W. A. Heterogeneity in presynaptic regulation of GABA release from hippocampal inhibitory neurons. *Neuron* 11: 1057–1067, 1993.

LARSON, J. AND LYNCH, G. Role of *N*-methyl-D-aspartate receptors in the induction of synaptic potentiation by burst stimulation patterned after the hippocampal $\theta$-rhythm. *Brain Res.* 441: 111–118, 1988.

LIPOWSKY, R., GILLESSEN, T., AND ALZHEIMER, C. Dendritic $Na^+$ channels amplify EPSPs in hippocampal CA1 pyramidal cells. *J. Neurophysiol.* 76: 2181–2191, 1996.

LUHMANN, H. J. AND PRINCE, D. A. Postnatal maturation of the GABAergic system in rat neocortex. *J. Neurophysiol.* 65: 247–263, 1991.

MAGEE, J. C. AND JOHNSTON, D. Characterization of single voltage-gated $Na^+$ and $Ca^{2+}$ channels in apical dendrites of rat CA1 pyramidal neurons. *J. Physiol. (Lond.)* 487: 67–90, 1995.

MAGEE, J. C. AND JOHNSTON, D. A synaptically controlled, associative signal for Hebbian plasticity in hippocampal neurons. *Science* 275: 209–213, 1997.

MAINEN, Z. F., CARNEVALE, N. T., ZADOR, A. M., CLAIBORNE, B. J., AND BROWN, T. H. Electrotonic architecture of hippocampal CA1 pyramidal neurons based on three-dimensional reconstructions. *J. Neurophysiol.* 76: 1904–1923, 1996.

MAJOR, G. Solutions for transients in arbitrary branching cables. III. Voltage clamp problems. *Biophys. J.* 65: 469–491, 1993.

MARKRAM, H., LUBKE, J., FROTSCHER, M., AND SAKMANN, B. Regulation of synaptic efficacy by coincidence of postsynaptic APs and EPSPs. *Science* 275: 213–215, 1997.

MILES, R., TÓTH, K., GULYÁS, A. I., HÁJOS, N., AND FREUND, T. F. Differences between somatic and dendritic inhibition in the hippocampus. *Neuron* 16: 815–823, 1996.

MOTT, D. D. AND LEWIS, D. V. Facilitation of the induction of long-term potentiation by $GABA_B$ receptors. *Science* 252: 1718–1720, 1991.

NEHER, E. Correction for liquid junction potentials in patch clamp experiments. In: *Methods in Enzymology*, Academic Press, 1992, p. 123–131.

PEARCE, R. A. Physiological evidence for two distinct $GABA_A$ responses in rat hippocampus. *Neuron* 10: 189–200, 1993.

PEARCE, R. A., GRUNDER, S. D., AND FAUCHER, L. D. Different mechanisms for use-dependent depression of two $GABA_A$-mediated IPSCs in rat hippocampus. *J. Physiol. (Lond.)* 484: 2: 425–435, 1995.

PRICE, J. L. An autoradiographic study of complementary laminar patterns of termination of afferent fibers to the olfactory cortex. *J. Comp. Neurol.* 150: 87–108, 1973.

PUIA, G., COSTA, E., AND VICINI, S. Functional diversity of GABA-activated $Cl^-$ currents in Purkinje versus granule neurons in rat cerebellar slices. *Neuron* 12: 117–126, 1994.

RALL, W. AND SEGEV, I. Space-clamp problems when voltage clamping branched neurons with intracellular microelectrodes. In: *Voltage and Patch-Clamping With Microelectrodes*, edited by T. G. Smith, Jr., H.

Lecar, and S. J. Redman. Bethesda, MD: Am. Physiol. Soc. 1985, p. 191–215.

SATOU, M., MORI, K., TAZAWA, Y., AND TAKAGI, S. F. Interneurons mediating fast postsynaptic inhibition in pyriform cortex of the rabbit. *J. Neurophysiol.* 50: 89–101, 1983.

SCHWINDT, P. C. AND CRILL, W. E. Amplification of synaptic current by persistent sodium conductance in apical dendrite of neocortical neurons. *J. Neurophysiol.* 74: 2220–2224, 1995.

SPRUSTON, N., JAFFE, D. B., WILLIAMS, S. H., AND JOHNSTON, D. Voltage- and space-clamp errors associated with the measurement of electrotonically remote synaptic events. *J. Neurophysiol.* 70: 781–802, 1993.

STALEY, K. J., SOLDO, B. L., AND PROCTOR, W. R. Ionic mechanisms of neuronal excitation by inhibitory $GABA_A$ receptors. *Science* 269: 977–981, 1995.

STEWARD, O., TOMASULO, R., AND LEVY, W. B. Blockade of inhibition in a pathway with dual excitatory and inhibitory action unmasks a capability for LTP that is otherwise not expressed. *Brain Res.* 516: 292–300, 1990.

SVOBODA, K., DENK, W., KLEINFELD, D., AND TANK, D. W. In vivo dendritic calcium dynamics in neocortical pyramidal neurons. *Nature* 385: 161–165, 1997.

TRAUB, R. D., JEFFERYS, J.G.R., MILES, R., WHITTINGTON, M. A., AND TOTH, K. A branching dendritic model of a rodent CA3 pyramidal neurone. *J. Physiol. (Lond.)* 481: 79–95, 1994.

TRAUB, R. D., MILES, R., AND WONG, R.K.S. Models of synchronized hippocampal bursts in the presence of inhibition. I. Single population events. *J. Neurophysiol.* 58: 739–751, 1987.

TSENG, G.-F. AND HABERLY, L. B. Characterization of synaptically mediated fast and slow inhibitory processes in piriform cortex in an in vitro slice preparation. *J. Neurophysiol.* 59: 1352–1376, 1988.

TSUBOKAWA, H. AND ROSS, W. N. IPSPs modulate spike backpropagation and associated $[Ca^{2+}]_i$ changes in the dendrites of hippocampal CA1 pyramidal neurons. *J. Neurophysiol.* 76: 2896–2906, 1996.

WIGSTRÖM, H. AND GUSTAFSSON, B. Facilitated induction of hippocampal long-lasting potentiation during blockade of inhibition. *Nature* 301: 603–604, 1983.

ZHANG, D. X. AND LEVY, W. B. Bicuculline permits the induction of long-term depression by heterosynaptic, translaminar conditioning in the hippocampal dentate gyrus. *Brain Res.* 613: 309–312, 1993.